

Fabrication and Characterization of Zeolite ZSM-12@MOF-74 Nanoporous Coordination Polymer Nanocomposite for removal of environmental toxic substances

Azita Albouyeh

Azad University

Afshin Pourahmad (✉ pourahmad@iaurasht.ac.ir)

Azad University <https://orcid.org/0000-0003-2007-8991>

Hassan Kefayati

Azad University

Research Article

Keywords: ZSM-12, Catalysis, Nanoporous, Pollution, Inorganic polymer chemistry, Wastewater

Posted Date: March 31st, 2021

DOI: <https://doi.org/10.21203/rs.3.rs-361844/v1>

License: © ⓘ This work is licensed under a Creative Commons Attribution 4.0 International License.

[Read Full License](#)

Abstract

White rice husk silica (RHS) was used as a silica source for ZSM-12 (MTW) zeolite synthesis. The ZSM-12 zeolite derived from RHS was prepared by hydrothermal method at 150°C. MOF-74(Zn) metal-organic framework (MOF) as a shell was grown over zeolite ZSM-12 as a core at room temperature. The ZSM-12@MOF-74 core@shell was used as a visible light driven photocatalyst for degradation of methylene blue (MB). The materials were characterized using a range of techniques. The ZSM-12@MOF-74 core@shell indicated the highest photocatalytic activity. Degradation mechanism was attributed to electrons and holes are generated in the organic ligand. The core@shell was extremely stable during five cycle test and did not demonstrate any explicit loss of photocatalytic activity during five cycle tests. The used adsorbent can be reused for adsorptive removal through simply washing.

1 Introduction

Recently, because of the rapid development of several of dyeing wastewater are leaved into the environment directly without adequate treatments [1]. The toxicity of industrial dyes inflicts a serious hazard to the water environment and human health [2]. Synthetic dyes from printing and dyeing industries prevent sunlight penetration into water and cause the death of plants and animals, as well as are harmful to humans [3]. Accordingly, efficient treatment technologies such as photocatalytic oxidation or reduction, membrane filtration, biological treatment, and adsorption have been developed for the removal of organic dyes from wastewater [4]. Recently, advanced oxidation processes (AOPs) have been widely considered due to chemical stability, recovery, and high efficiency in removing pollutants from water sources [5]. Zeolites and MOFs are two important examples of nanoporous materials. Zeolite and MOF have common specifications of high surface areas and uniform micropores and differ in thermal/mechanical stability and structural flexibility. The integration of MOF and zeolite into composite particles is envisaged to produce useful hybrid nanoporous where inorganic zeolite and organic MOF components transmit the advantages of high thermal, mechanical and structural stability of zeolites and specific functionality and high flexibility of MOFs [6]. There are a few reports on zeolite@MOF composites [7–10]. Recently, we reported synthesis of Zeolite Y @ MIL-53 (Al) core@shell [11], with modifying of zeolite Y surface with COOH groups. In this study, Zeolite Socony Mobil-12 (ZSM-12) and MOF-74 were chosen as components in the zeolite@MOF core@shell for photoregradation of MB as a cationic dye. RHS was used as a silica source for ZSM-12 zeolite synthesis [12]. Zn-MOF-74 is a typical MOF with high density of metal sites and high stability for heterogeneous catalysis [13]. MOF-74 (Zn) has been chosen as the target photocatalyst owing to its stability, low cost, nontoxic nature and visible light response [14]. MOF-74 (Zn) containing transition metals as structural nodes are expected to be semiconductors since the empty d metal orbitals mixed with the LUMOs of the organic linkers form the conduction band [15]. Herein, we report the photocatalytic activity of ZSM-12@MOF-74 (Zn) in photodegradation of MB dye.

2 Experimental

All materials were prepared from Merck or Sigma-Aldrich. The RH for synthesis of ZSM-12 was collected at a local rice milling plant in the State of Guilan, Iran. The ZSM-12 from RHS was synthesized by hydrothermal method with some modification in the described procedure in our previous literature [12]. The chemical composition of the initial gel was: $1.96\text{Na}_2\text{O}:27\text{SiO}_2:\text{Al}_2\text{O}_3:5\text{TEA}_2\text{O}:240\text{H}_2\text{O}$. The ZSM-12-COOH was synthesized based on described procedure in literature [8]. The MOF-74 was obtained through the hydrothermal synthesis in described procedure in the literature [16]. For preparing of ZSM-12@MOF-74 core@shell, 0.5 g of ZSM-12-COOH was added to the synthesis mixture of MOF-74 and the mixture was stirred for 24 h. Then product was washed and dried at room temperature. In order to delete any possible linker covering the pores of the MOF-74, the solid product was cleaned with DMF. The photocatalytic activities of the products were determined by the decomposition of azo dye containing MB in the aqueous solution. 2 mg of photocatalysts was diffused into 50 mL of the MB dye solution (10 mg L^{-1}), and magnetically stirred in the dark for about 30 min to make sure the solidification of adsorption-desorption equilibrium. Then it was exhibited to visible light irradiation to initial the reaction. The removal and degradation yield were measured with respect to the change in intensities of absorption peaks at 664 nm (λ_{max} of MB dye). The powder X-ray diffraction patterns of the samples were recorded using an X-ray diffractometer (X Pert Prompd) with Cu K α radiation ($\lambda = 1.545\text{ \AA}$). The transmission electron micrographs (TEM) were recorded with a Philips CM10 microscope. Scanning electron microscope (SEM) was conducted with a TESCAN MIRA3 scanning electron microscope operated at 30 kV. The specific surface area and pore diameter were measured using a Sibata Surface Area Apparatus 1100. The UV-Vis diffused reflectance spectra (UV-Vis DRS) were obtained with a UV-Vis Scinco 4100 spectrometer with an integrating sphere reflectance accessory. The infrared spectra (FT-IR) were measured on a Bruker spectrophotometer using KBr pellets. The zeta potential (ζ) was measured using a streaming potential analyzer (Zhejiang Circle-Tech Membrane Technology Co., Ltd, China).

3 Results And Discussion

The XRD pattern of the synthesized samples is shown in Fig. 1. The XRD pattern of MOF-74 (Zn) (Fig. 1a) and zeolite ZSM-12 (Fig. 1b) was matched quite well with pattern that were given in articles [16]. Both of them possess very good crystallinity. The XRD pattern of the ZSM-12@MOF-74 core@shell (Fig. 1c) indicated diffraction peaks that had been ascribed to separate MOF-74 and zeolite ZSM-12. But the intensity of ZSM-12 peaks was very low with respect to single zeolite ZSM-12. It can be due to proper covering of zeolite ZSM-12 by MOF-74 shells. The results were in agreement with other articles [17].

Nanoparticle morphology was observed for MOF-74 (Zn) (Fig. 2a). The average particle size was 25 nm. The SEM micrographs of the parent ZSM-12 (Fig. 2b) clearly show aggregates with average width of $\sim 1\text{ }\mu\text{m}$ and thickness of $\sim 500\text{ nm}$. Detailed observation of the surface of the crystals proves rougher surface for the parent zeolite. The SEM image of core@shell indicated agglomerates of small nanoparticles of MOF-74 that covered all surfaces of zeolite ZSM-12 core. The EDX spectra of the core@shell sample (insert in Fig. 2c) show that the ZSM-12@MOF-74 contained all elements. O, C, Al, Si, and Zn elements were homogeneously distributed in the core@shell. Figure 2d shows a conventional TEM image of the

nanosized MOF-74 crystals. The estimation of the average crystal size was ~ 22 nm, in good agreement with the Scherrer equation valuation from XRD peak broadenings (27 nm). TEM image of the ZSM-12@MOF-74 (Fig. 2f) consisted of two regions. One dark region related to zeolite ZSM-12 with average width of ~ 200 nm and length of ~ 400 nm and light part with an average diameter of 10 nm that related to MOF-74 shell.

The FT-IR spectrum of carboxylic groups of ZSM-12 (Fig. 3a) as core indicated Si–O–Si bending and stretching vibrations at 1098, 804 and 486 cm^{-1} . The band at 3464 cm^{-1} belongs to acidic bridged hydroxyls in the ZSM-12-COOH. The presence of peaks around $1650\text{--}1700\text{ cm}^{-1}$ nm is related to carboxylic groups. The FT-IR spectrum of the ZSM-12@MOF-74 core@shell (Fig. 3c) is an amalgamation of both materials (MOF-74 and ZSM-12). The bridging hydroxyl groups of the MOF-74, (Zn–OH–Zn), was appeared around 3360 cm^{-1} along with a shoulder at 3710 cm^{-1} . The carbonyl (–C = O) stretching vibration of linker was observed at 1550 cm^{-1} in spectra. The carboxyl groups of the ligand that was coordinated to the metal centers show adsorption peak at 1650 cm^{-1} .

The DR spectra of the ZSM-12 and ZSM-12@MOF-74 core@shell are indicated in Fig. S1A. The adsorption edges for ZSM-12 and ZSM-12@MOF-74 core@shell were about 350 and 520 nm with band gap energy (E_g) about 3.54, and 2.38 eV, respectively. The DR spectrum showed that core@shell was able to absorb visible light. N_2 adsorption/ desorption isotherms of the synthesized samples, are shown in Fig. S1B. MOF-74 (Zn) and ZSM-12@MOF-74 core@shell depicted type IV with a hysteresis loop which confirms the presence of mesoporous structures. The BET surface area of the MOF-74 and ZSM-12@MOF-74 core@shell, calculated from the adsorption isotherm over $P/P_0 = 0.05\text{--}0.15$, are 750 and 980 $\text{m}^2\text{ g}^{-1}$, respectively. The larger surface area provides more active centers and more contact area to promote the yield and selectivity of a specific reaction.

Table 1 shows adsorption and degradation of MB by prepared catalysts at pH 3, 7 and 9. The zeta potential results indicated the pH_{PZC} of MOF-74(Zn), ZSM-12 and ZSM-12@MOF-74 core@shell were 2.8, 2.2 and 4.8, respectively. The synthesized catalysts possess high adsorption capacity and degradation at $\text{pH} > 5$ due to the electrostatic interaction between catalysts negative surface charge and cationic MB dye. The removal of cationic dye on MOF-74 and core@shell was more than ZSM-12. This action might mention that electrostatic interaction is not the significant way to control the adsorption capacity of MOF-74 and ZSM-12@MOF-74 to cationic dye. Based on structure of MB dye and MOF-74, $\pi - \pi$ stacking interaction as another force controlled the removal of MB on core@shell and MOF-74 [9]. The highest percentage of destruction was obtained (47.55% degradation and 80.37% removal) using ZSM-12@MOF-74 compared to those of MOF-74 (36.15% degradation) and zeolite ZSM-12 (18.35% degradation) at $\text{pH} = 9$. Under visible light, the excitation of valence bond electrons of MOF-74 occurs and eventually active radicals for degradation of MB dye are produced. Electrons and holes in the organic ligand are generated with energy larger than the energy gap between HOMO and LUMO orbitals. Electrons pass through ZnO5 to operate with O_2 to produce H_2O_2 and finally hydroxyl radical ($\cdot\text{OH}$). The produced holes in organic ligand can directly react with MB dye, water molecules or hydroxyl ion (OH^-) to generate hydroxyl radical.

The photosatbility of the ZSM-12@MOF-74 photocatalyst was retained at ~ 67.87% removal of MB dye even after five successive experimental runs under the same conditions (Fig. S2a). Therefore, the photocatalyst can be suitable for its practical applications in environmental remediation. The XRD pattern of ZSM-12@MOF-74 core@shell after of irradiation, indicated in Fig. S2b. The minor differences are observed in the intensity of some diffraction, but they indicate similar framework structures.

Table 1

The photocatalytic performances of the MOF-74(Zn) and ZSM-12@MOF-74, $C_{\text{OMB}} = 10$ ppm, the photocatalyst dosage: 0.4 g/L, at 30 min dark and 30 min under visible light irradiation.

Sample	Adsorbed dye ^a (%)	Degraded dye ^b (%)	Removed dye ^c (%)
MOF-74 (pH = 3)	14.40	23.23	37.63
MOF-74 (pH = 7)	21.23	35.75	56.98
MOF-74 (pH = 9)	28.98	36.15	65.13
ZSM-12 (pH = 3)	9.32	7.38	16.70
ZSM-12 (pH = 7)	17.54	15.27	32.81
SZM-12 (pH = 9)	20.51	18.35	38.86
ZSM-12@MOF-74 (pH = 3)	15.64	35.47	51.11
ZSM-12@MOF-74 (pH = 7)	28.72	46.74	75.46
ZSM-12@MOF-74 (pH = 9)	32.87	47.50	80.37
^a Determined with UV-vis after 30 min of stirring in dark.			
^b Determined with UV-vis after 30 min of irradiation with visible-light.			
^c The total amount of dye removed after 60 min of reaction.			

4 Conclusion

The ZSM-12 zeolite derived from RHS was prepared by hydrothermal method at 150°C in the presence of tetraethylammonium hydroxide. Metal –organic framework type of MOF-74 as a shell was growth over zeolite ZSM-12 as a core by solvothermal method. Synthesized ZSM-12@MOF-74 core@shell can remove MB cationic dye in aqueous solution under visible light irradiation. The TEM and SEM images demonstrated core@shell structure from ZSM-12 as a core and MOF-74 as a shell. MB dye was adsorbed on core@shell by electrostatic interaction and $\pi - \pi$ stacking interaction. The removal of MB dye by synthesized core@shell, MOF-74 and ZSM-12 was 80.37, 47.50 and 18.37 % at pH = 9, respectively.

Declarations

Acknowledgments

The authors are grateful to the Islamic Azad University, Rasht Branch.

References

1. Y. An, H. Zheng, Z. Yu, Y. Sun, Y. Wang, C. Zhao, W. Ding, Functioned hollow glass microsphere as a self-floating adsorbent: Rapid and high-efficient removal of anionic dye. *J. Hazard. Mater.* **381**, 120971 (2020)
2. A. Sh. Sohrabnezhad, M. Pourahmad, Fallah, Karimi, Magnetite-metal organic framework core@shell for degradation of ampicillin antibiotic in aqueous solution. *J. Solid State Chem.* **288**, 121420 (2020)
3. M. Kaykhaii, M. Sasani, S. Marghzari, Removal of dyes from the environment by adsorption process. *Chem. Mater. Eng.* **6**, 31 (2018)
4. M. Naimi Joubani, M.A. Zanjanchi, Sh. Sohrabnezhad, The carboxylate magnetic – zinc based metal-organic framework heterojunction: $\text{Fe}_3\text{O}_4\text{-COOH@ZIF-8/Ag/Ag}_3\text{PO}_4$ for plasmon enhanced visible light z-scheme photocatalysis. *Adv. Powd. Technol.* **31**, 29 (2020)
5. S. Sh. Sohrabnezhad, Daraie Mooshangaie, In situ fabrication of n-type Ag/AgBr nanoparticles in MCM-41 with rice husk (RH/MCM-41) composite for the removal of Eriochrome Black-T. *Mater. Sci. Eng. B.* **240**, 16 (2019)
6. G. Zhu, R. Graver, L. Emdadi, B. Liu, K.Y. Choi, D. Liu Synthesis of Zeolite@Metal Organic Framework Core-Shell Particles as Bifunctional Catalysts. *RSC Adv.* **4**, 30673 (2014)
7. K. Tanaka, T. Muraoka, D. Hirayama, A. Ohnishi, Highly efficient chromatographic resolution of sulfoxides using a new homochiral MOF–silica composite. *Chem. Commun.* **48**, 8577 (2012)
8. Y. Song, D. Hu, F. Liu, S. Chen, L. Wang, Fabrication of fluorescent $\text{SiO}_2\text{@zeolitic imidazolate framework-8}$ nanosensor for Cu^{2+} detection. *Analyst.* **140**, 623 (2015)
9. D.-W. Lim, H. Lee, S. Kim, I.H. Cho, M. Yoon, Y.N. Choi, An unprecedented single platform via cross-linking of zeolite and MOFs. *Chem. Commun.* **52**, 6773 (2016)
10. X. Pan, H. Xu, X. Zhao, H. Zhang, Metal–Organic Framework-Membranized Bicomponent Core–Shell Catalyst HZSM-5@UIO-66- NH_2 /Pd for CO_2 Selective Conversion. *ACS Sustainable Chem. Eng.* **8**(2), 1087 (2020)
11. F. Azadi, A. Pourahmad, Sh Sohrabnezhad, M. Nikpassand, Synthesis of Zeolite Y@ metal–organic framework core@shell. *J. Coord. Chem.* **73**(24), 3412 (2020)
12. A. Gh. Mehmandoust, Pourahmad, Preparation of ZSM-12 Zeolite from RHS and Its Application for Synthesis of n-type ZnO Semiconductor Nanoparticles: A Green Chemistry Approach. *J. Inorg. Organomet. Polym. Mater.* **28**, 2213 (2018)

13. P.J. Jodłowski, G. Kurowski, K. Dymek, R.J. Jędrzejczyk, P. Jelen, Ł. Kuterasiński, A. Gancarczyk, A. Węgrzynowicz, T. Sawoszczuk, M. Sitarz, In situ deposition of M (M = Zn; Ni; Co)-MOF-74 over structured carriers for cyclohexene oxidation - Spectroscopic and microscopic characterization. *Microporous Mesoporous Mater.* **303**, 110249 (2020)
14. V.T. Thuy Nguyen, C.L. Luu, T. Nguyen, A. Phung Nguyen, C. Tien Hoang, A. C. Ha, Multifunctional Zn-MOF-74 as the gas adsorbent and photocatalyst. *Adv. Nat. Sci. Nanosci. Nanotechnol.* **11**, 035008 (2020)
15. C.G. Silva, A. Corma, H. García, Metal-organic frameworks as semiconductors. *J. Mater. Chem.* **20**, 3141 (2010)
16. D.J. Tranchemontagne, J.R. Hunt, O.M. Yaghi, Room temperature synthesis of metal-organic frameworks: MOF-5, MOF-74, MOF-177, MOF-199, and IRMOF-0. *Tetrahedron.* **64**, 8553 (2008)
17. N.L. Rosi, J. Kim, M. Eddaoudi, B. Chen, M. O'Keeffe, O.M. Yaghi, Rod Packings and Metal - Organic Frameworks Constructed from Rod-Shaped Secondary Building Units. *J. Am. Chem. Soc.* **127**, 1504 (2005)

Figures

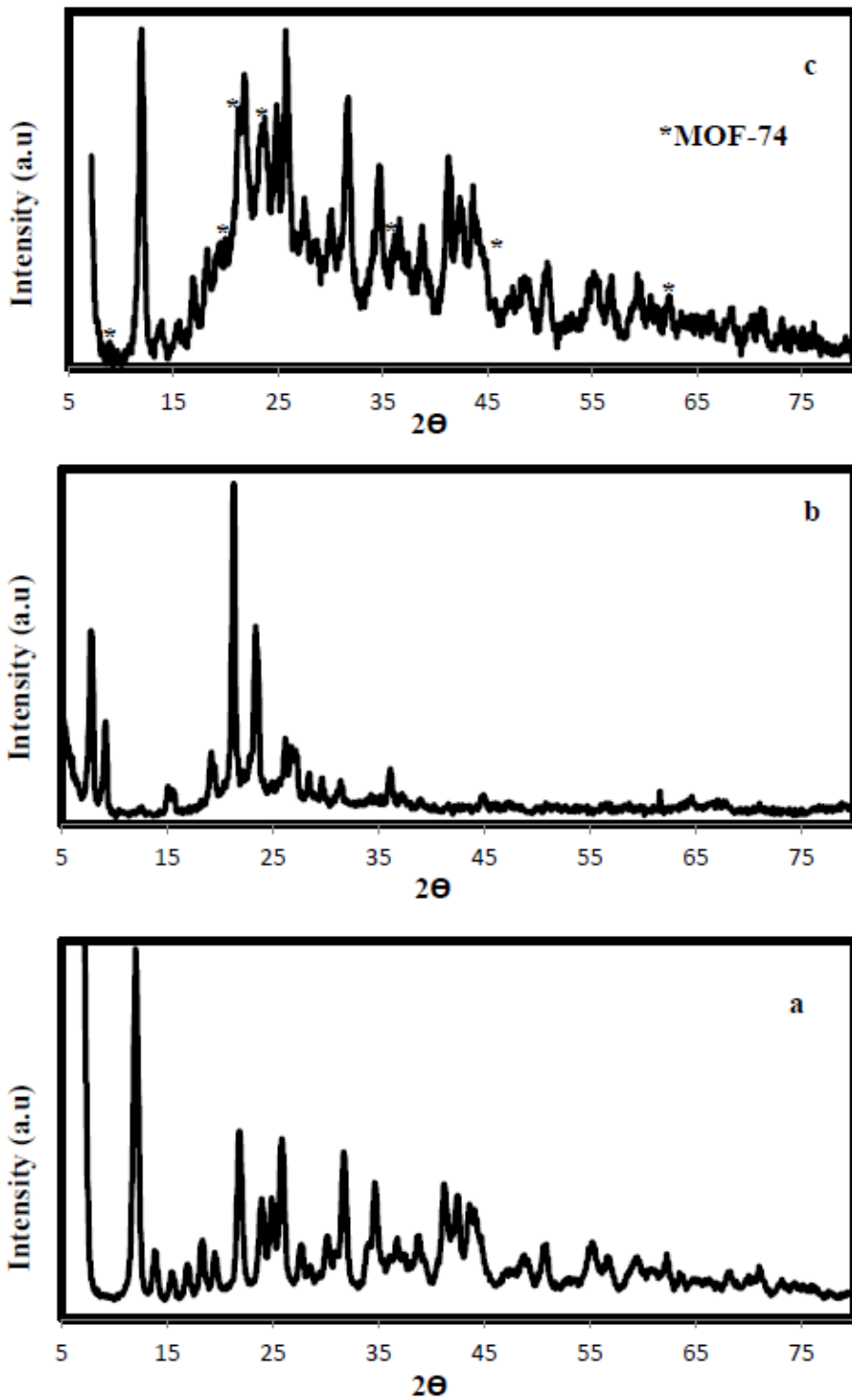


Figure 1

XRD patterns of (a) MOF-74 (Zn), (b) Zeolite ZSM-12 and (c) ZSM-12@MOF-74

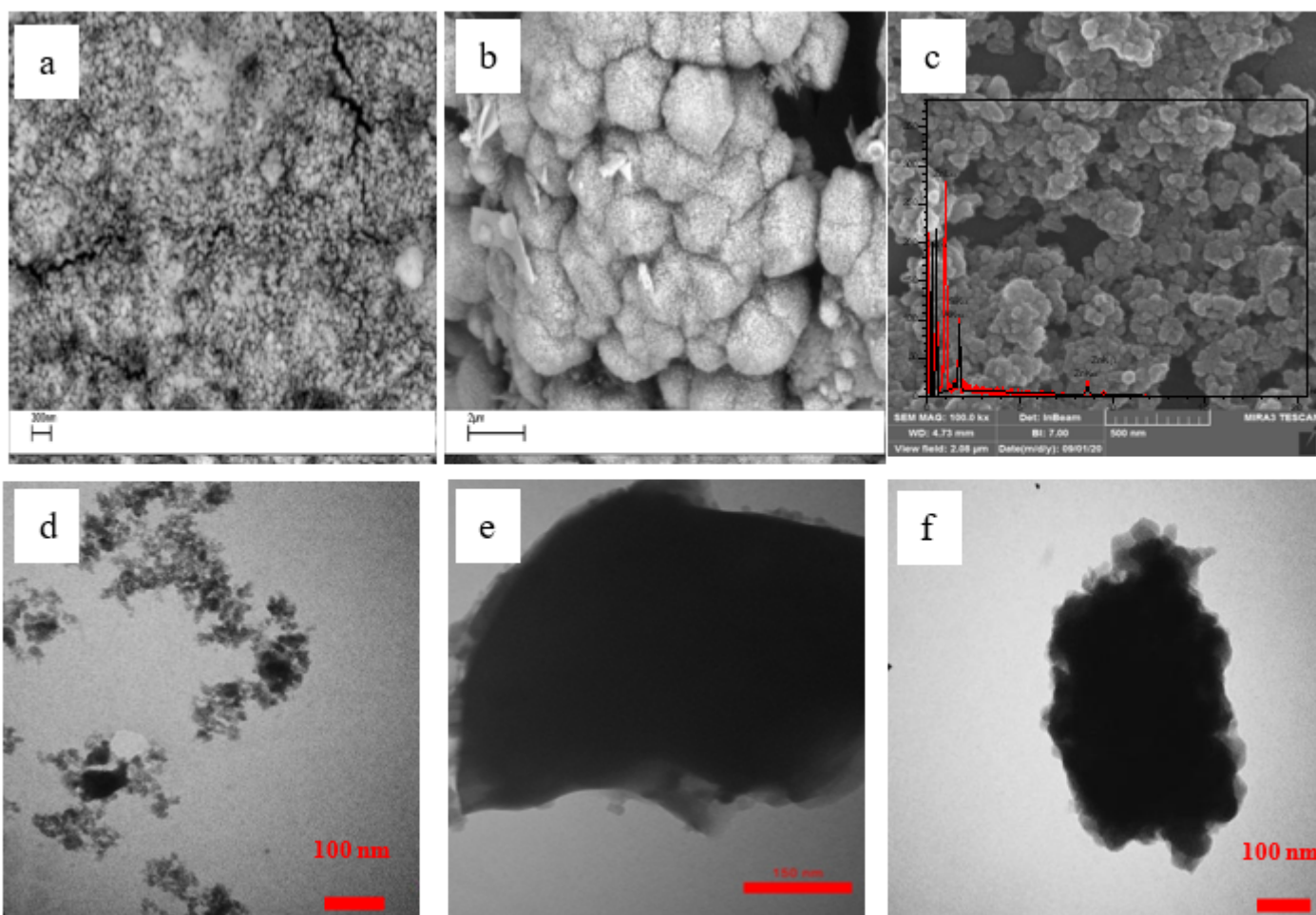


Figure 2

SEM images of (a) MOF-74 (Zn), (b) zeolite ZSM-12, (c) ZSM-12@MOF-74 along with EDX result, and TEM images of (d) MOF-74 (Zn), (e) zeolite ZSM-12 and (f) ZSM-12@MOF-74 samples.

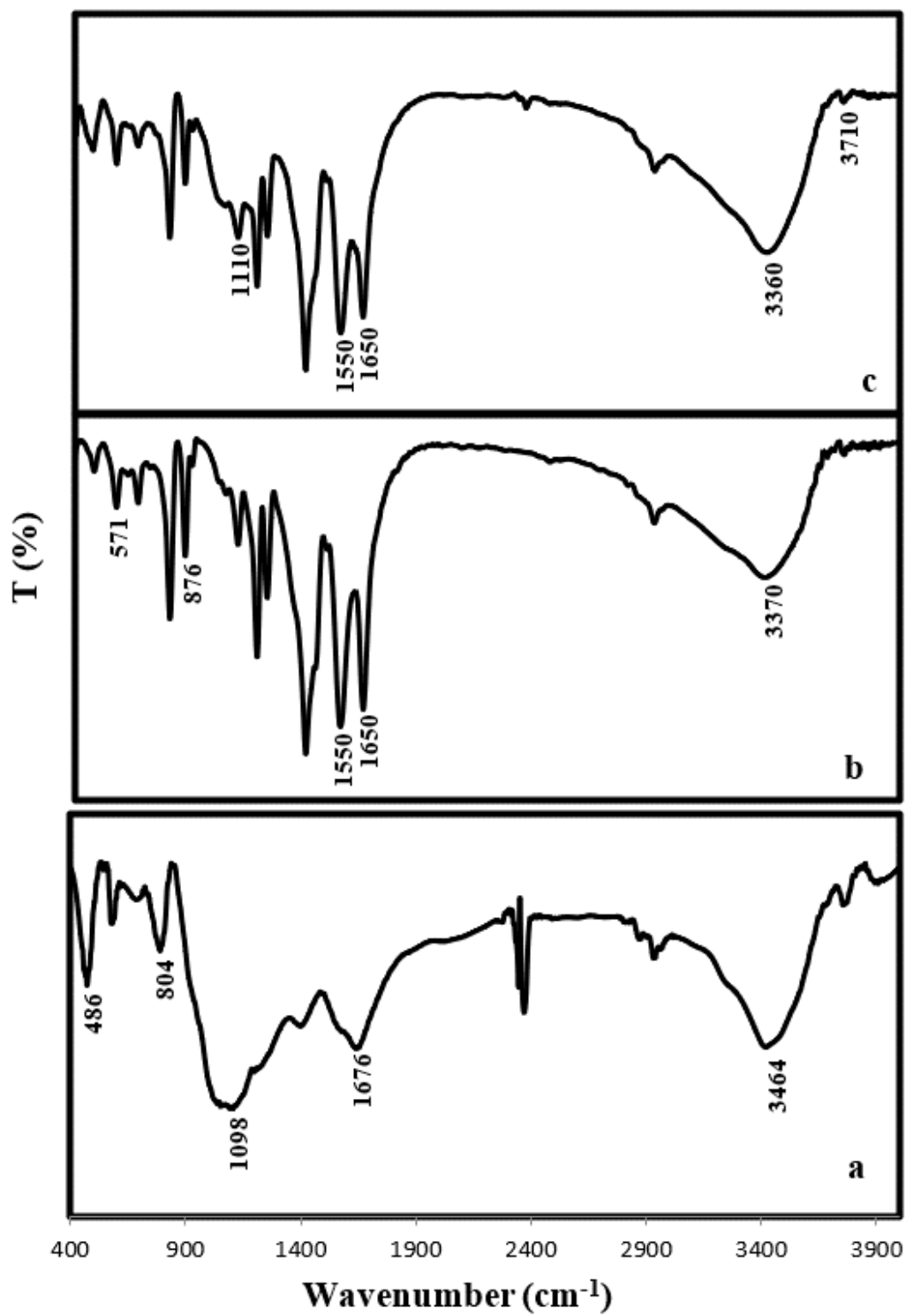


Figure 3

FT-IR spectra of (a) ZSM-12-COOH, (b) MOF-74 (Zn) and (c) ZSM-12@MOF-74.

Supplementary Files

This is a list of supplementary files associated with this preprint. Click to download.

- [GraphicalAbstract.docx](#)
- [FigureS1.docx](#)
- [FigureS2.docx](#)
- [SupportingInformation.docx](#)